2950 Niles Road, St. Joseph, MI 49085-9659, USA
269.429.0300 fax 269.429.3852 hq@asabe.org www.asabe.org

An ASABE Meeting Presentation

Paper Number: 083897

Effect of Wind Tunnel Air Velocity on VOC Flux Rates from CAFO Manure and Wastewater

David B. Parker, Edward Caraway, Marty Rhoades, Chanci Donnell, Jan Spears

West Texas A&M University, Canyon, Texas

N. Andy Cole, Richard W. Todd

USDA-ARS, Bushland, Texas

Kenneth D. Casey

Texas AgriLife Research, Texas A&M System, Amarillo, Texas

Written for presentation at the
2008 ASABE Annual International Meeting
Sponsored by ASABE
Rhode Island Convention Center
Providence, Rhode Island
June 29 – July 2, 2008

Abstract. *Wind tunnels and flux chambers are often used to measure volatile organic compound (VOC) emissions and estimate emission factors from animal feeding operations (AFOs) without regard to air velocity or sweep air flow rates. Laboratory experiments were conducted to evaluate the effect of wind tunnel air velocity on VOC emission rates. VOC emissions were measured on standard solutions of VOCs in water, and on manure and wastewater from beef cattle and dairy AFOs at wind tunnel air velocities between 0.003 and 0.2 m/s corresponding to volumetric air exchange rates of 0.6 to 39 exchanges per minute. Activated-carbon-filtered air was passed through a small rectangular wind tunnel (30.5 cm length, 15.2 cm width, 5.1 cm height). Outlet air was sampled using stainless steel sorbent tubes (Tenax® TA) and analyzed for seven volatile fatty acids (acetic, propionic, isobutyric, butyric, isovaleric, valeric, hexanoic) and four heavier molecular weight (MW) semi-VOCs (phenol, p-cresol, indole and skatole) using gas chromatography/mass spectrometry. VOC emission rates increased linearly with increasing wind velocity. These results show that wind velocity is a major factor affecting VOC emissions from AFOs. Selection of representative air velocity or sweep air flow rate is critical when estimating VOC emission factors using wind tunnels and flux chambers.*

Keywords. odor, flux chamber, wind tunnel, emission rates, emission factors, volatile fatty acids, phenolic, indolic, gas chromatography

The authors are solely responsible for the content of this technical presentation. The technical presentation does not necessarily reflect the official position of the American Society of Agricultural and Biological Engineers (ASABE), and its printing and distribution does not constitute an endorsement of views which may be expressed. Technical presentations are not subject to the formal peer review process by ASABE editorial committees; therefore, they are not to be presented as refereed publications. Citation of this work should state that it is from an ASABE meeting paper. EXAMPLE: Author's Last Name, Initials. 2008. Title of Presentation. ASABE Paper No. 08----. St. Joseph, Mich.: ASABE. For information about securing permission to reprint or reproduce a technical presentation, please contact ASABE at rutter@asabe.org or 269-429-0300 (2950 Niles Road, St. Joseph, MI 49085-9659 USA).

Introduction

Volatile organic compounds (VOCs) are emitted from wastewater treatment plants, food processing plants, landfills, and animal feeding operations (AFOs) (Kim et al., 2006). VOCs are produced from the degradation of amino acids in the intestines of humans and animals (Mackie et al., 1998) and from incomplete anaerobic digestion (Mata-Alvarez et al., 2000). Sunesson et al. (2001) identified 70 VOCs from dairies in Sweden using sorbent tubes and GC/MS, with *p*-cresol, 2-butanone, ethyl acetate, α-pinene and Δ3-carene found at the highest concentrations. Filipy et al. (2006) identified 73 VOCs emitted from a dairy lagoon. Rabaud et al. (2002, 2003) identified 35 VOCs emitted from California dairies.

VOC emissions are an important aspect of air quality for two reasons: 1) many VOCs are malodorous (Rabaud et al., 2002, 2003; Parker et al., 2007; Wright et al., 2005) and 2) some VOCs are photochemically reactive and are precursors to the formation of ozone, a regulated air pollutant (Aquino et al., 2007; Carter, 1994). The United States Environmental Protection Agency (U.S. EPA) has defined "reactive VOCs" as any compound of carbon which participates in atmospheric photochemical reactions and lists those that are not included as reactive such as CO, CO_2, methanes and ethanes in 40CFR51.100s (U.S. EPA, 1995a).

The quantification of VOC emissions from AFOs is important not only for estimation of emission factors from a regulatory standpoint, but also to determine which sources emit VOCs so that best management practices can be developed for reducing emissions and odors. There are several approaches to estimating emission rates: 1) the mass balance approach where source concentrations are measured over time and the difference is used to determine losses to the atmosphere, 2) indirect methods where ambient concentrations are measured and source emission rates are backcalculated using dispersion models, and 3) direct methods where emission rates are measured directly from the source using a wind tunnel or flux chamber (Hudson and Ayoko, 2008a; NAS, 2003). The mass balance approach is often preferred, but instances are few, especially for VOC emissions from large area sources, where the mass balance approach can be used in field conditions. Each of these methods has advantages and disadvantages that depend on the particular project.

As part of ongoing research to quantify VOC emissions from AFOs, and in an attempt to increase the knowledge base concerning measurement of VOC emissions with wind tunnels and flux chambers, several experiments were conducted to evaluate how wind velocity affects emission rates of VOCs found at beef cattle feedyards and dairies. The specific objectives were to 1) quantify the effect of wind velocity on VFA and semi-VOC emission rates, and 2) evaluate the importance of Henry's law constant on emission rate predictions using the various two-film models.

Literature Review

There has been a long-standing debate about the appropriateness and accuracy of wind tunnels and flux chambers for quantifying emissions at AFOs and other area sources (Hudson and Ayoka, 2008a; Hudson and Ayoka, 2008b; Zhang et al., 2002; Lindberg et al., 2002; Rhoades et al., 2005; Cole et al., 2007; Fowler et al., 2001; Ryden and Lockyer, 1985; Meisinger et al., 2001; Watkins et al., 1972; Whitehead and Rastrick, 1991; Kissel et al., 1977).

Many scientists have recognized that wind velocity and air flow across soil and water surfaces affects the flux of ammonia and some VOCs (Liss and Slater, 1974; Delos et al., 1984; Mills et al., 1985; Wanninkhof, 1992; Zahn et al., 1997; Zhang et al., 2002; Lindberg et al., 2002; Bidleman and McConnell, 1995; Eklund, 1992; Leyris et al., 2005). When measuring ammonia

emissions in simulated retention pond and feedlot surfaces, Cole et al. (2007) found that emission rates in a flux chamber at 0.5 exchanges per minute were less than 25% of that from an open surface. At an operating hog farm, Zahn et al. (1997) found that VOC emissions downwind of a swine manure storage basin increased with wind speed between 0.2 and 9.4 m/s, with a maximum emission rate at 3.6 m/s.

There have been several approaches to estimating the mass transfer of VOCs, one of which is the two-film model.

The Two-Film Model

The conventional two-film volatilization model, once called the "stagnant film model," has been used for describing volatilization of a solvent-solute mixture (Liss and Slater, 1974; Sadek et al., 1996; Bianchi and Varney, 1997). Much of the earlier research with the two-film model was related to estimating gas exchange over the ocean (Wanninkhof, 1992). The two-film model can be conceptually described by the diagram in Figure 1.

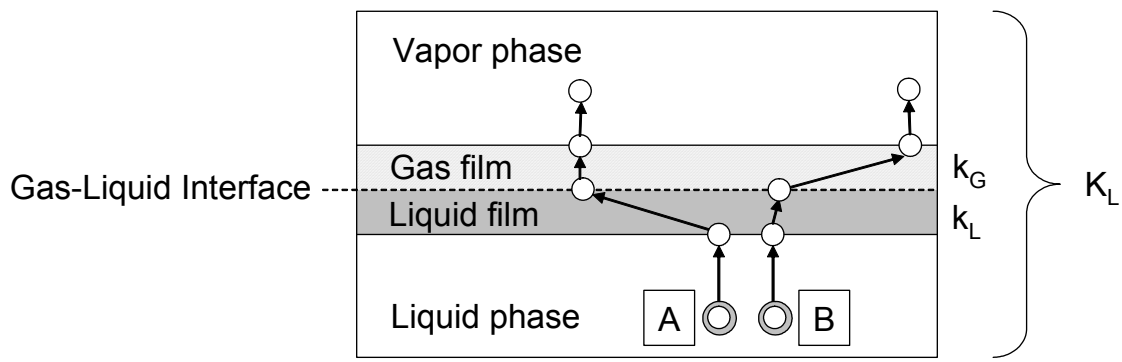

Figure 1. Conceptual diagram of the two-film model.

As a VOC moves from the liquid phase to the vapor phase, it must pass through two films, the liquid film and the gas film. If a VOC molecule is liquid film limited, then conceptually its path will follow that of molecule A in Figure 1, whereas if it is gas film limited it will follow the path of molecule B. Hudson and Ayoko (2008a) provides further discussion on this topic.

The volatilization flux through these two films is defined as

$$J = k_L(C_L - C_L^*) = k_G(C_G^* - C_G) \qquad [1]$$

where J=flux (mass/area-time); k_L is the liquid-film transfer coefficient (length/time); k_G is the gas-film transfer coefficient (length/time), C_L is the VOC concentration in the liquid phase (mass/volume); C_G is the VOC concentration in the vapor phase; C_L^* is the VOC concentration in the liquid film and C_G^* is the VOC concentration in the gas film. Because C_L^* and C_G^* cannot be measured directly, Eq. 1 has been simplified assuming $C_G^* = H_{cc}\ C_L^*$ to obtain

$$J = K_L(C_L - C_G/H_{cc}) \qquad [2]$$

where K_L is the overall solute transfer coefficient and H_{cc} is the dimensionless Henry's constant discussed in more detail later. K_L is calculated using the equation

$$K_L = \frac{k_L k_G H_{cc}}{k_L + k_G H_{cc}} \quad [3]$$

If the VOC concentration in air (C_G) is small such that it does not inhibit the VOC flux, then Eq. 2 can be simplified to the following

$$J = K_L (C_L - C_G / H_{cc}) \cong K_L (C_L) \quad [4]$$

Note that the Eq. 4 approximation is only valid when $C_G / H_{cc} << C_L$. On the other extreme, the flux will be zero (suppressed by the elevated gas concentration) when $C_G = C_L \ H_{cc}$.

Empirical correlations for estimating k_L and k_G have been proposed based on values for reference compounds as summarized in Lee et al. (2004):

$$k_L = k_L^R \left(\frac{M_R}{M} \right)^{1/2} \quad [5]$$

$$k_G = k_G^R \left(\frac{M_R}{M} \right)^{1/2} \quad [6]$$

where k_L^R is the reference liquid-film transfer coefficient (i.e. oxygen) and k_G^R is the reference gas-film transfer coefficient (i.e. water vapor); M_R and M are the respective molecular weights of the reference substance (oxygen=32 and water=18) and the solute or VOC. The k_L^R of oxygen (0.2 m/hr) and the k_G^R of water vapor (30 m/hr), are often used for estimating k_L and k_G of the solute.

Henry's Law Constants

Henry's law constants can be expressed in a variety of units as mass per volume per pressure (i.e. mg L^{-1} atm^{-1} or M atm^{-1}). Henry's law constant is often presented in its dimensionless form H_{cc} as

$$H_{cc} = \frac{C_{air}}{C_{water}} \quad [7]$$

where C_{air} is the concentration in air (mass/volume) and C_{water} is the concentration in water (mass/volume) (Sawyer and McCarty, 1978; Buonicore and Davis, 1992). In this form, Henry's law states that, at equilibrium, the VOC concentration in the air is directly proportional to the VOC concentration in the water. Henry's law constants are temperature specific. Henry's law constants for several VOCs found at AFOs are presented in Table 1.

Table 1. Dimensionless Henry's law constants for several VOCs emitted from animal feeding operations.		
Analyte	Molecular Weight (g/mol)	Henry's Law Constants at 20-25°C
Acetic acid	60.0	7.6E-06 [(a)]
Propionic acid	74.2	8.3E-06 [(a)]
Isobutyric acid	88.1	1.2E-05 [(a)]
Butyric acid	88.1	1.2E-05 [(a)]
Isovaleric acid	102.1	3.4E-05 [(a)]
Valeric acid	102.1	1.9E-05 [(a)]
Hexanoic acid	116.2	3.2E-05 [(a)]
Phenol	94.1	2.6E-05 [(a)]
p-Cresol	108.1	2.7E-05 [(a)]
Indole	117.1	2.45E-06 [(b)]
Skatole	131.2	8.70E-05 [(c)]
a) From Hudson and Ayoko (2008a) b) From Anon (2002) c) From Abu-Khalaf and Iversen (2007)		

Methods of Incorporating Wind Velocity into the Two-Film Model

As summarized by Bianchi and Varney (1997), the earlier stagnant film model (Liss and Slater, 1974) was recognized to significantly underestimate emission rates of some VOCs, primarily because of the failure to take into account wind velocity effects. Recognizing that wind velocity was a key element in VOC emission rates, several empirical methods were subsequently developed for incorporating wind velocity into the two-film model. Mills et al. (1985) and Delos et al. (1984) presented an equation for estimating k_G which takes into account the effect of wind speed:

$$k_G = 170\left(\frac{18}{M}\right)^{1/4} V \qquad [8]$$

with k_G in m/d and V in m/s. Though the height of the wind speed is not always mentioned, most scientists have used either the 2 m or 10 m height (Wanninkhof, 1992).

Lee et al. (2004) introduced the "β concept" for calculating k_G which includes an empirically determined turbulence factor based on the velocity in the wind tunnel:

$$k_G = \beta\left(\frac{RT}{2M_R\pi}\right)^{1/2} \quad [9]$$

where β is an empirical factor determined through laboratory experiments with a small wind tunnel that accounts for the efficiency of a vapor moving into air. A major finding was that β was almost the same for different VOCs. A graph of β vs. air velocity (V) is shown in Figure 2. Velocities were measured at a height of 4.5 cm above the water surface. Lee found the sharpest increase in β between 0 and 0.2 m/s, which is within the range of velocities used in our current research.

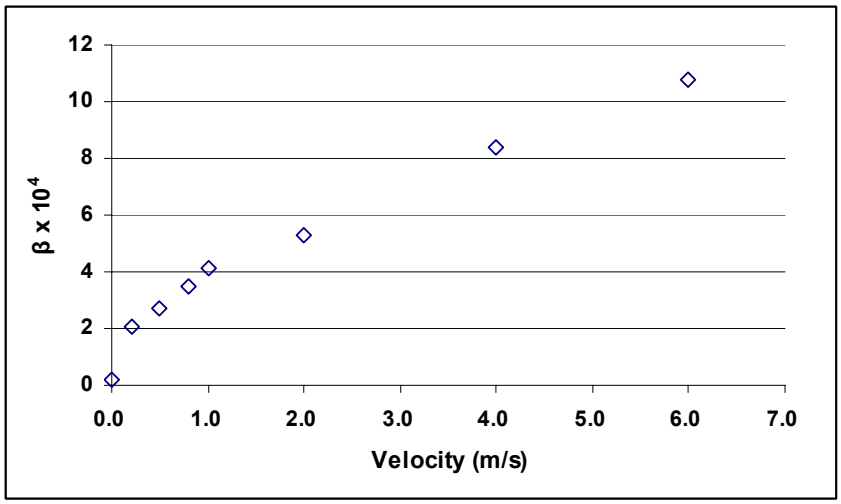

Figure 2. Relationship between β and air velocity (from Lee et al., 2004). Note that the air velocity was measured at 4.5 cm height above the water surface.

The Importance of Henry's Law Constant and Wind Velocity on Emissions of AFO VOCs

In a project developed at EPA's Atmospheric Reseach and Exposure Assessment Laboratory, Gholson et al. (1989; 1991) evaluated the flux chamber method for measuring VOC emissions from quiescent liquid surfaces, and stated that "varying the sweep flow rate was found to have little effect on the measured emission rate between 2 L/min and 10 L/min." This research has led some scientists to believe that flux chambers are appropriate for measuring all VOCs, including those at animal feeding operations. However, it is important to note that the VOCs Gholson measured were those typically found in landfills and other industrial facilities. As shown in Table 2, those VOCs have much higher Henry's law constants (H_{cc}) than the VOCs typically found in animal feeding operations. With the exception of acetone and 1-butanol, the VOCs have H_{cc} values that make them liquid film controlled as opposed to the VOCs at AFOs which are gas film controlled. When H_{cc} is greater than 1.0×10^{-3}, then the VOCs are liquid film controlled, and VOCs that are liquid film controlled are not affected by wind velocity (Lee et al., 2004; Schwarzenbach et al., 2003; Liss and Slater, 1974; Hudson and Ayoka, 2008a). Thus,

while Gholson's conclusion was appropriate for the majority of VOCs that he measured (Table 2), his conclusions are not appropriate for VOCs found at CAFOs (Table 1).

Table 2. Dimensionless Henry's law constants for several VOCs emitted from landfills and industrial facilities.

Analyte	Molecular Weight	Henry's Law Constants at 20-25°C [(a)]
1,1,1-Trichloroethane	133.4	6.82×10^{-1}
Methyl ethyl ketone	72.1	2.05×10^{-2}
Benzene	78.1	2.27×10^{-1}
Toluene	92.1	2.73×10^{-1}
o-xylene	106.2	2.15×10^{-1}
Acetone	58.1	1.64×10^{-3}
1-Butanol	74.1	2.92×10^{-5}
Tetrachloroethylene	165.8	1.02

a) From Sander, 1999

To demonstrate the importance of Henry's law constants and wind velocity effects, the two-film model with the Mills et al. (1985) velocity correction (Eq. 8) was used to calculate and compare emission rates from typical VOCs found at AFOs (such as acetic acid and phenol) with those found at industrial and landfill facilities (such as 1,1,1-trichlorethane and tetrachloroethylene). To show the hypothetical effect on a single graph, in the model simulations the initial concentrations in water were set to 400 mg/L for acetic acid and phenol, and 10 mg/L for 1,1,1-trichlorethane and tetrachloroethylene. Wind velocities were varied from 0.1 to 2.0 m/s. As shown in Figure 3, the two-film model demonstrates that wind velocity has a great effect on emissions of compounds like acetic acid and phenol with small H_{cc}, while wind velocity has little effect on emissions of compounds with large H_{cc} like 1,1,1-trichlorethane and tetrachloroethylene.

Materials and Methods

Wind Tunnel Design

Traditional wind tunnels are designed for uniformity of airflow both longitudinally and transversely. With typical wind velocities of 0.5 to 2.0 m/s, corresponding exchange rates of 30 to 120 exchanges/min are achieved for a one-meter long test section. Unlike traditional wind tunnels, the wind tunnel in this research was designed to simulate some physical aspects of the U.S. EPA-type flux chamber (i.e. air is distributed into the flux chamber through small, equally-spaced holes) yet provide for the ability to measure and/or calculate longitudinal wind velocities which cannot be done in the U.S. EPA-type flux chamber. Because the U.S. EPA-type flux chamber uses low volumetric exchange rates (i.e. 0.167 exchanges/min at a sweep air flowrate of 5 L/min), the wind tunnel in this research was designed to operate at lower exchange rates and velocities than traditional wind tunnels.

The small rectangular wind tunnel used in this research had dimensions of 5.1 cm height, 30.5 cm length, and 15.2 cm width (Figure 4), with a surface area of 0.046 m^2 and cross-sectional area of 0.0062 m^2 (based on an operating height of 4.1 cm allowing for 1 cm inset into the water or other media). The wind tunnel was constructed of 5 cm square steel tubing and 4.4x4.4 cm angle iron with a 5 mm thick Plexiglas top. To simulate the physical aspects of the U.S. EPA flux chamber, air was dispersed into the wind tunnel through six 5-mm diameter holes equally spaced in the steel tubing at a height 2 cm above the emitting surface (Figure 4). Air exited the tunnel through three 1.3 cm diameter holes in the Plexiglas top at the opposite end of the tunnel.

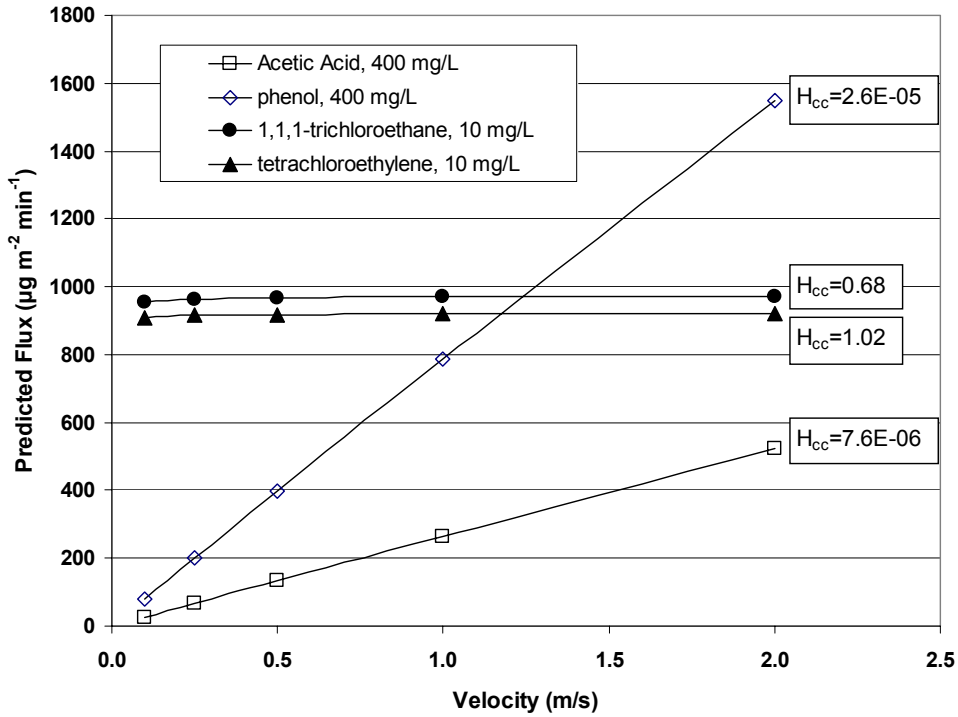

Figure 3. Emission rates predicted using the two-film model demonstrating the effect of wind velocity at 2 m height on VOCs with differing Henry's law constants (H_{cc}).

Manure or liquid samples were placed in a shallow pan of dimension slightly greater than the wind tunnel to a depth of 1 cm, and the wind tunnel was placed over the pan. The sweep air was supplied from a laboratory air compressor. The sweep air was passed through an activated carbon filter to remove any VOCs in the compressed air, then through a rotameter and into the wind tunnel. The sweep air flowrate was controlled using one of three valved rotameters selected for low, medium, or high flowrates (Cole Parmer N102-05, 0-3.9 L/min; Gilmont GF-6541-1230, 0-25 L/min; Gilmont 127 mm, 0-500 L/min). In the experiments, sweep air flowrates ranged between 1.1 to 75 L/min, corresponding to sweep air velocities of 0.003 to 0.2 m/s and sweep air volumetric exchange rates of 0.6 to 39 exchanges/min. Actual air velocities leaving the small 5-mm diameter holes ranged from 0.156 m/s at the lowest sweep air flowrate of 1.1 L/min, to 10.6 m/s at the highest sweep air flowrate of 75 L/min. This compares to air velocities leaving the holes of 0.29 m/s for a sweep air flowrate of 5 L/min in the U.S. EPA flux chamber (Eklund, 1992). At this flowrate, the wind speed in the U.S. EPA flux chamber has been

described as “still, but not stagnant” (Eklund, 1992). The wind tunnel designed for this research had air velocities leaving the holes that encompassed that of the U.S. EPA flux chamber (0.156 to 10.6 m/s as compared to 0.29 m/s), and overall sweep air exchange rates greater than that of the U.S. EPA flux chamber (0.6 to 39 exchanges/min as compared to 0.167 exchanges/min).

After leaving the rotameter, the sweep air entered the wind tunnel at one end, passed over the emitting surface, then exited at the opposite end. At a given sweep air velocity, three volumetric exchanges of sweep air were passed through the wind tunnel prior to VOC sampling. Samples were collected at the lowest velocity first, moving to the highest velocity to minimize potential effects of decreasing VOC concentration in the source.

Air samples were collected from air as it exited the middle hole in the Plexiglas top. A fraction of the air exiting the wind tunnel was sampled using stainless steel sorbent tubes (90 mm x 5 mm I.D., SKC Inc.) filled with either a single bed 150 mg Tenax TA® 60/80 adsorbent or a dual-bed adsorbent consisting of 150 mg Tenax TA® 60/80 and 100 mg of Carbopack BAW 6.6% Carbowax 80/120 adsorbent.

Figure 4. Photograph of the small wind tunnel used in the research. Air entered the wind tunnel through the small holes in the upper right, and exited through the holes at the lower left.

Air was pulled through the sorbent tubes at 200 mL/min using a portable vacuum pump (SKC Inc.). Sampling time ranged from 5 to 15 min depending on source concentration, with a target sampling volume of 1.0 to 3.0 L per sample. The entire measurement process generally took 90 minutes or less to collect air samples over three to five velocities on a single source.

Gas Chromatography/Mass Spectrometry

Sorbent tube samples were analysed using a Varian® 3800/Saturn 2000 gas chromatagraph/ mass spectrometer (GC/MS) and two methods. For method 1, the GC/MS was equipped with a Varian WCOT Fused Silica, 25 m x 0.25 mm ID, CP-Wax 58 column. Sorbent tube samples were desorbed using a Perkin-Elmer® automated thermal desorber (ATD) where the sorbent tube samples were desorbed at 225°C for 15 minutes, trapped in a quartz cryotrap at -30°C,

then the trap was heated to 225°C and desorbed into the GC/MS. The column oven was ramped from 60°C to 230°C at 6°C per minute for a total run time of 30.3 minutes.

For method 2, the GC/MS was equipped with an HP-Innowax Fused Silica, 30 m x 0.25 mm ID column and sorbent tube samples were desorbed using a Markes Unity® automated thermal desorber. The column oven was held at 35°C for 2 minutes, then ramped from 35°C to 230°C at 6°C per minute for a total run time of 38 minutes.

Samples were analyzed for four semi-VOCs (phenol, p-cresol, indole, skatole) and seven VFAs (acetic, propionic, isobutyric, butyric, isovaleric, valeric, hexanoic).

Standards and Method Detection Limits

Standards for the semi-VOCs were prepared in methanol, and VFA standards were prepared in hexanes. All standards and solvents were FCC Kosher grade (>99% purity) purchased from Sigma Aldrich. Standards were prepared using serial dilutions, then 1 to 10 µL of the standards were injected onto clean tubes using a calibration solution loading rig (CSLR™, Markes International). The liquid calibration standard was introduced through the injector septum in argon carrier gas using a standard GC syringe, then analyzed using the same GC/MS method used for the field samples. For the VFAs, standard curves were made from six standards with one replicate at each concentration. In addition, seven replicates were conducted at two of the concentrations to aid in calculation of method detection limits. For the semi-VOCs, the standard curves were made from eight standards with seven replicates at each concentration. Linear regression was used for all curves, passing through the origin. A typical standard curve for p-cresol on sorbent tubes is shown in Figure 5. Coefficients of determination (R^2) for the standard curves ranged from 80 to 99% for the seven VFAs, and from 95 to 98% for the four semi-VOCs.

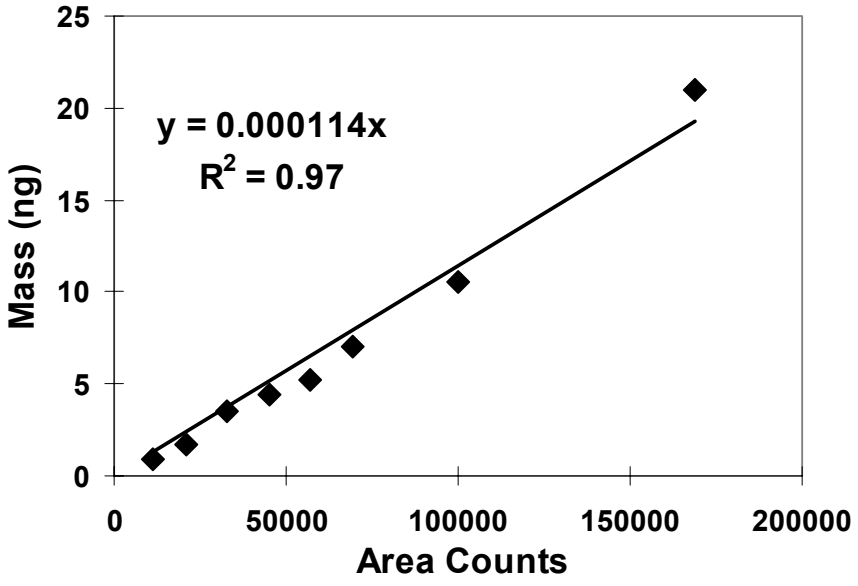

Figure 5. A typical standard curve (p-cresol) used for quantification of ambient VOC concentrations. Each point is the average of seven replications.

Method detection limits (MDLs) were calculated per U.S. EPA guidelines as the product of the standard deviation of seven replicates and the student's *t*-value at the 99% confidence level (U.S. EPA, 1999; U.S. EPA, 1995b). For seven replicates (6 degrees of freedom), a *t*-value of 3.14 was used.

The MDL was calculated in mass (ng) then converted to a reportable MDL in ng/L. Whenever the calculated MDL was less than the minimum standard for that compound, the minimum standard was reported as the MDL. Method detection limits are presented in Table 3.

Source Samples

Emission rates were measured on the following standard solutions and source samples:

1. Standard solutions of acetic acid and phenol at concentrations of 20 mg/L and 200 mg/L in water.
2. One source sample of beef cattle manure collected from the pen surface of the 600 head West Texas A&M University beef cattle research feedyard (30% moisture content, wet weight basis),
3. One source sample of runoff holding pond effluent collected from a 50,000 head commercial beef cattle feedyard,
4. Three source samples of anaerobic treatment and storage lagoon wastewater from a 3,000 cow commercial dairy.

All source samples had been previously frozen. Source samples were thawed overnight in sealed containers and allowed to reach equilibrium with laboratory room temperature of 21.1°C.

Emission (evaporation) rates of distilled water were also quantified at varying wind velocities in the wind tunnel.

Table 3. Range of masses used in the standards and method detection limits for each compound.

	Standards	MDL
	Min-max (ng)	(ng/L)
Acetic acid	1.9-75	16.8
Propionic acid	1.0-40	13.8
Butyric acid	2.5-100	33.9
Isobutyric acid	1.5-60	16.2
Isovaleric acid	0.06-2.5	0.51
Valeric acid	0.6-25	5.7
Hexanoic acid	25-1000	564
Phenol	1.2-30	3.75
P-cresol	0.9-21	2.64
Indole	0.5-12	1.5
Skatole	0.25-6	0.75

Calculation of Emission Rate

Flux density (i.e. flux rate) was calculated on a mass per unit area per unit time using Eq. 10

$$E_{WT} = \frac{CQ}{A_{WT}} \qquad [10]$$

where E_{WT} = wind tunnel flux rate for analyte (μg m^{-2} min^{-1}), C = concentration of component measured in the exit air (μg L^{-1}), Q = sweep air flow rate (L min^{-1}), and A_{WT} = surface area enclosed by the wind tunnel (m^2).

Results and Discussion

Measured Emission Rates from Standard Solutions

Flux rates vs. wind velocity for 20 mg/L and 200 mg/L solutions of phenol in water showed strong linear relationships at both concentrations (Figure 6). Similar linear trends were observed for standard solutions of acetic acid in water (not shown).

Measured Water Evaporation Rates from the Wind Tunnel

Chao et al. (2005) presented measured k_G^R values for distilled water under various wind speeds measured at a height of 4.5 cm in a wind tunnel (Table 4).

Table 4. Values of k_G^R for distilled water under tested wind velocity (from Chao et al., 2005).

Wind velocity (m/s)*	0	0.2	0.5	0.8	1.0	2.0	4.0	6.0
k_G^R (cm/min)	10.9	72	102	129	143	191	284	359
k_G^R (m/day)	157	1037	1469	1858	2059	2750	4090	5170

*Velocity measured at height of 4.5 cm above water surface

Using the data of Chao et al. (2005), and a linear relationship for wind speeds between 0 to 0.2 m/s as measured at 4.5 cm above the water surface, k_G^R and wind speed would be related by the following equation:

$$k_G^R = 157 + 4400\ V \qquad [11]$$

with k_G^R in m/day and V in m/s. Chao's values of k_G^R increased 6.6-fold between wind velocities of 0.0 and 0.2 m/s.

Using the two-film model with k_G^R values from Eq. 11, and negating any inhibitive effects from water vapor (i.e. the evaporation rate approaches zero at 100 percent relative humidity), values of actual evaporation were plotted against predicted evaporation rates from the wind tunnel (Figure 7). Because the relative humidity was not measured, the effect of water vapor could not be included.

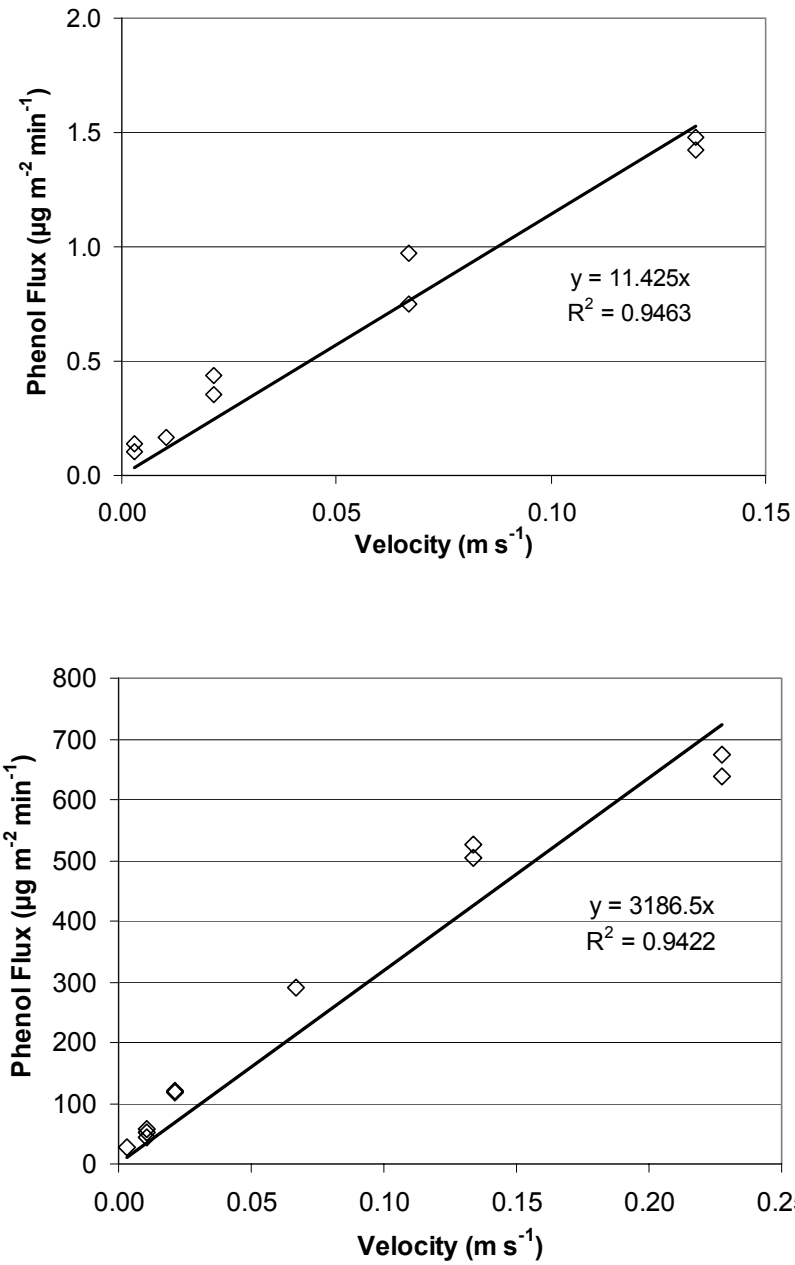

Figure 6. Graphs showing the relationship between measured flux and wind velocity at 2 cm height for standard solutions of phenol in water at 20 mg/L (top) and 200 mg/L (bottom).

As shown in Figure 7, the linear approximation for k_G^R between 0 and 0.2 m/s of Eq. 11 adapted from Chao et al. (2005) leads to a decent approximation of actual evaporation for evaporation rates of 4.0E+6 µg m^{-2} min^{-1} and above, corresponding to wind velocities of 0.0388 m/s and above and exchange rates of 6.3 exchanges/minute and above.

Given the measured evaporation rates and negating any effects from water vapor concentrations in the air, the respective k_G^R values as a function of wind speed, which were back calculated from the two-film model for the wind tunnel used in this research, are presented in Table 5. The best fit regression model for the data in Table 5 was:

$$k_G^R = -24322\ V^2 + 10039\ V \qquad (R^2=0.981) \qquad [12]$$

with k_G^R in m/day and V in m/s

Our values of k_G^R increased 11.3-fold between wind velocities of 0.00267 and 0.1335 m/s, a greater increase than reported by Chao et al. (2005). There are three possible reasons for this increase: 1) our velocities were measured at 2 cm above the surface whereas Chao's were measured at 4.5 cm above the surface, 2) in Chao's experiments, the relative humidity of the ambient air was reported at 85 to 90%, whereas in our experiments the ambient relative humidity was 40-50%, and 3) we focused on velocities between 0 and 0.13 m/s whereas Chao's experiments ranged from 0 to 6.0 m/s.

One of the difficulties in comparing emission rates and wind velocity effects is the many different wind tunnel and flux chamber configurations. In a recent review paper, Hudson and Akoyo (2008b) summarized more than 50 different wind tunnel and flux chamber geometries. While comparison of emission rates can be difficult among the different wind tunnel geometries, the measurement of k_G^R values and distilled water evaporation rates would be one method useful for standardizing and comparing emission rates from the different geometries.

Measured Flux Rates from Source Samples

Typical graphs of flux rate vs. air velocity for acetic acid and phenol from three of the sources are shown in Figure 8. Similar trends were observed for all VOCs and all sources, with flux rates increasing with wind velocity. As shown in Figure 8, some of the flux-velocity relationships appeared quadratic at velocities less than 0.05 m/s, while others were more linear across the entire wind velocity range.

A summary of the slopes and coefficients of determination for each of the VOCs and sources is presented in Table 6. Most of the R^2 values were greater than 0.90, indicating a strong linear relationship between flux rate and wind velocity.

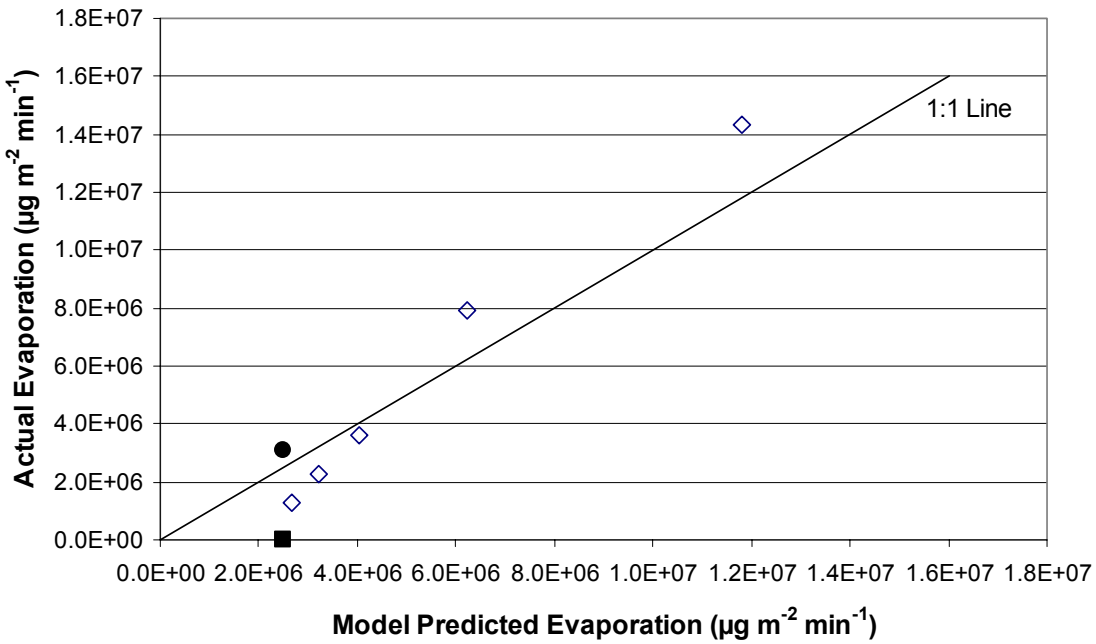

Figure 7. Measured evaporation rates vs. two-film model predicted evaporation rates using the k_G^R vs. wind speed of Chao et al. (2005) of Equation 11 (shown in diamonds). The solid circle is the measured evaporation rate from an open container in the laboratory (ventilated laboratory with minor air movement), while the solid square is the steady state evaporation rate of zero for a zero velocity closed system in the wind tunnel with 100% relative humidity. Note that the model did not account for the inhibition effects from increasing concentrations of water vapor at low velocities (high relative humidity reduces actual evaporation).

Table 5. Experimentally determined values of k_G^R for distilled water under tested wind velocity and exchange rate for the wind tunnel of this research.

Wind velocity (m/s)*	0.003	0.010	0.032	0.053	0.133
Air Exchange Rate (exchange volumes/minute)	0.58	2.05	6.31	10.5	26.3
k_G^R (cm/min)	5.5	9.9	15.7	34.7	62.7
k_G^R (m/day)	79.8	142.0	226.0	500.0	903.0

*Average velocity at height of 2.0 cm above water surface.

Determination of Appropriate Wind Tunnel Velocities to Simulate Field VOC Emissions at AFOs

As demonstrated in this research, wind velocity can have a great impact on emission rates of VOCs found at CAFOs. Thus, correct handling of wind velocity or sweep air flowrate is critical for estimating accurate and representative field-based emission rates.

There are two options for estimating representative field emission rates with wind tunnels:

Method 1: The wind velocity or air flow rate in the wind tunnel (or flux chamber) can be adjusted to match expected wind velocities in the field, or

Method 2: The emissions can be measured using a standard wind velocity or air flow rate and the emission rate can be scaled up or down based on expected wind velocities in the field.

Method 1 requires a prior knowledge about expected wind velocities before measurements are made in the field. Method 2 requires knowing the wind velocity vs. emission rate correlation for the specific wind tunnel or flux chamber, as the specific wind tunnel geometry and air flowrate determines the velocity at a given height above the measuring surface. Wind velocities in the field are typically measured at 2 or 10 m height, much higher than those in the wind tunnel. For a given roughness length, the logarithmic velocity profile can be calculated such that wind tunnel velocities at a given height can be correlated to equivalent velocities in the field at 2 or 10 m height. For a given velocity in the wind tunnel, the equivalent velocity at 2 or 10 m height is dependent on the surface roughness length, z_0.

To demonstrate how this procedure might be used for the wind tunnel used in this research, equivalent velocities at 2 and 10 m height were calculated using the logarithmic velocity profile (Ham, 2005) for roughness lengths of 0.0001 m for water and 0.01 m for manure (Eq. 13).

$$U_2 = U_1 * \ln (z_2/z_0) / \ln (z_1/z_0) \qquad [13]$$

where U_2=predicted velocity (m/s) at height z_2 (m), U_1=measured velocity (m/s) at height z_1 (m), and z_0=surface roughness length (m).

Accordingly, a wind tunnel velocity of 0.2 m/s (wind tunnel air flow rate of 75 L/min) corresponds to velocities at 2 m height of 0.37 and 1.53 m/s for the water and manure, respectively (Figure 9). Likewise, a wind tunnel velocity of 0.02 m/s (air flow rate 8 L/min) corresponds to velocities at 2 m height of 0.037 and 0.15 m/s for water and manure, respectively.

A Comparison of Measured Fluxes to Two-Film Modeled Fluxes

A comparison was made between measured fluxes of phenol (200 mg/L in water) at differing wind speeds, and fluxes as predicted by the two-film model both with and without various wind velocity corrections (Figure 10). The actual measured flux of phenol are denoted by the open diamonds and straight-line linear regression in Figure 10.

Table 6. Values of slope (m) and coefficient of determination (R^2) for dependent variable flux rate (µg m^{-2} min^{-1}) vs. independent variable wind velocity (m s^{-1}). All regressions were forced through the origin, giving the model: Flux Rate = m * wind velocity.

	Beef Manure		Beef Runoff Pond		Dairy Lagoon 1		Dairy Lagoon 2		Dairy Lagoon 3	
	m	R^2	m	R^2	m	R^2	M	R^2	m	R^2
Acetic	25.6	0.84	14.5	0.89	92.9	0.99	45.1	0.98	63.0	0.99
Propionic	16.3	0.68	6.7	0.63	30.4	0.99	4.89	0.73	7.8	0.97
Isobutyric	7.7	0.92	3.0	0.93	13.2	0.99	8.4	0.98	6.7	0.98
Butyric	341.7	0.92	102.4	0.66	412.6	0.99	31.7	0.04	73.8	0.98
Isovaleric	2.9	0.86	0.8	0.73	3.5	0.91	0.25	0.01	0.64	0.96
Valeric	84.2	0.95	34.0	0.94	131.2	0.96	8.4	0.46	12.0	0.91
Hexanoic	23.8	0.95	21.9	0.95	106.7	0.99	20.4	0.84	25.9	0.73
Phenol	64.1	0.91	35.1	0.77	3152.5	0.36	232.6	0.84	217.4	0.84
p-cresol	87.3	0.96	12.6	0.93	2918.0	0.79	497.4	0.94	256.5	0.71
Indole	20.1	0.99	3.7	0.95	295.6	0.93	57.0	0.89	18.8	0.71
Skatole	1.0	0.99	0.3	0.99	206.5	0.99	78.6	0.98	63.0	0.99

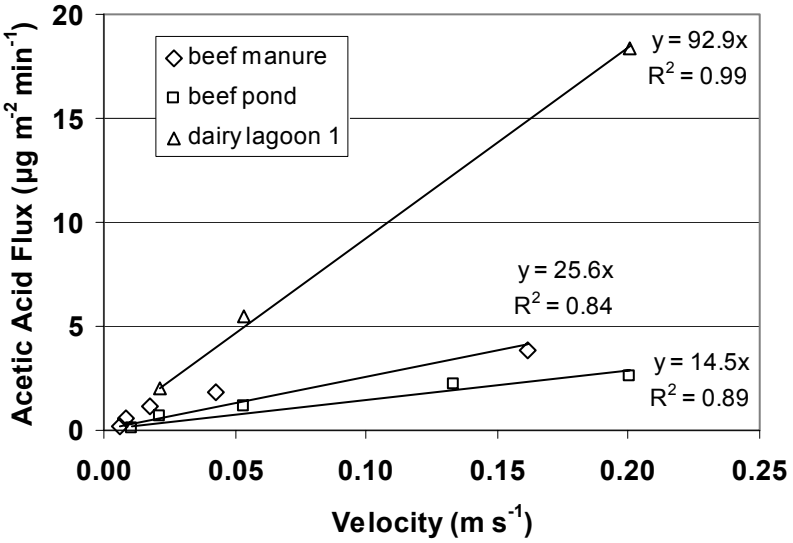

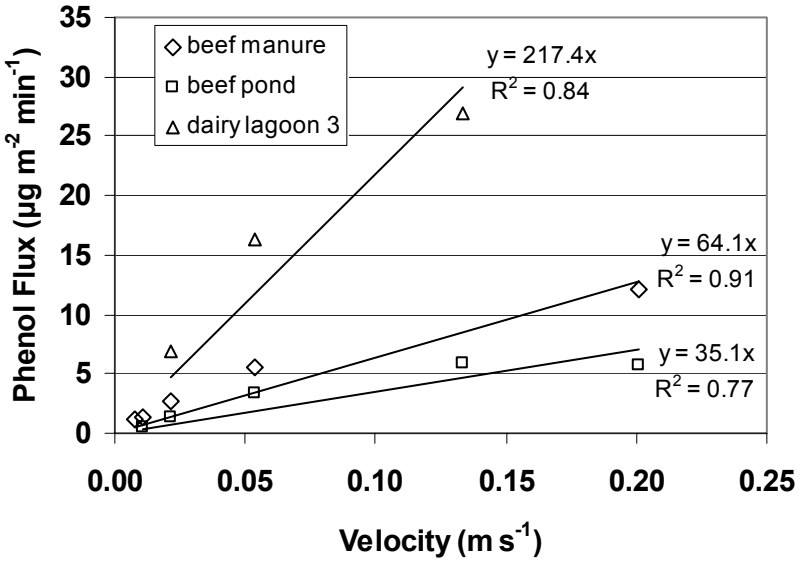

Figure 8. Graphs showing the relationship between measured flux and wind velocity at 2 cm height for acetic acid (top) and phenol (bottom) as measured on three AFO sources.

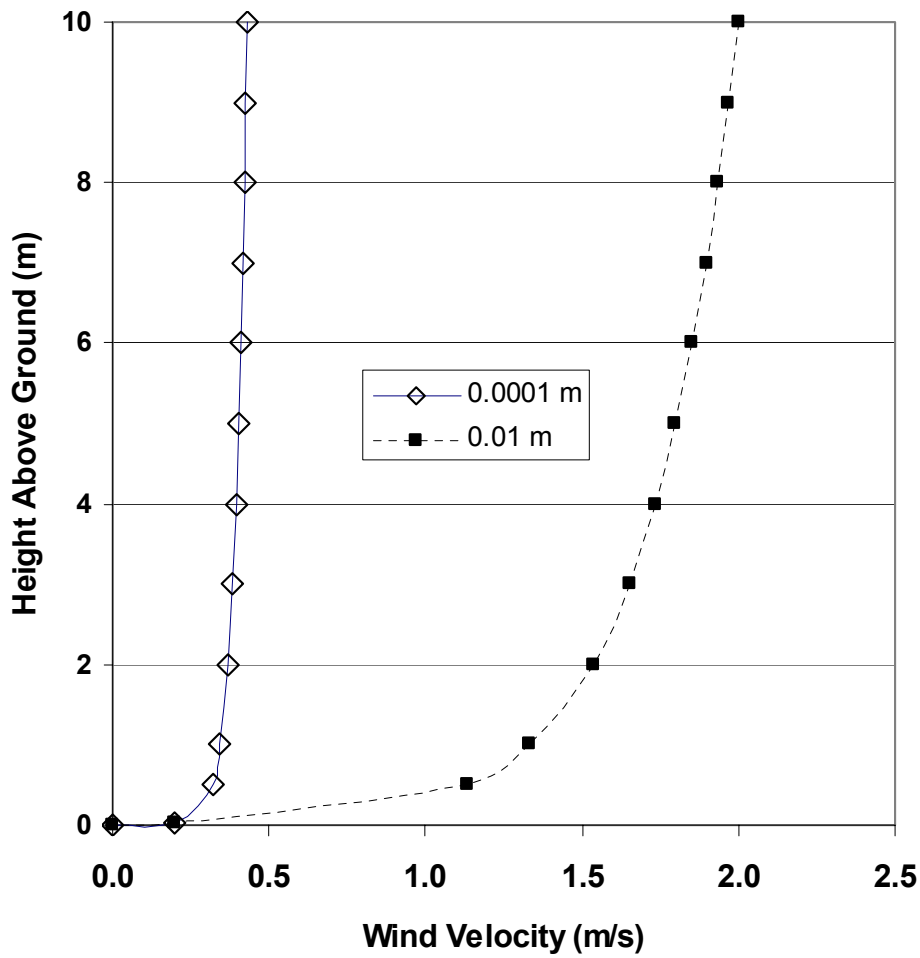

Figure 9. A comparison of logarithmic velocity profiles for surface roughness length (z_0) of 0.0001 m (water) and 0.01 m (manure). Both profiles simulate a wind tunnel velocity of 0.2 m/s at 2 cm height.

The two-film flux with Chao velocity correction was calculated using Eqs. 2, 3, and 5, but using Chao's k_G^R (Eq. 11) in Eq. 6 (denoted by the solid triangles in Figure 10). While the Chao velocity correction provided a better representation to how actual fluxes increase with velocity, the Chao correction provided flux estimates about 2.5 times the actual flux at the highest velocity.

The two-film flux with wind-tunnel specific k_G^R correction was calculated using Eqs. 2, 3, and 5, but using the wind-tunnel specific k_G^R measured in this research (Eq. 12, Table 5) (denoted by the open circles in Figure 10). While the specific k_G^R velocity correction provided a better fit near

the origin, like Chao's correction it overpredicted the actual phenol flux by about 2.2 times at the highest velocity (Figure 10).

The two-film flux with Mills velocity correction for K_G was calculated using Eqs. 2, 3, 5, and 8 (denoted by the solid circles in Figure 10). Because the Mills velocity correction formula (Eq. 8) uses a velocity at 2 m height, the velocity in the wind tunnel at 2 cm height was first converted to the velocity at 2 m height using Eq. 13. The Mills correction underpredicted the actual phenol flux. The predicted flux was about 25% of actual at the highest velocity.

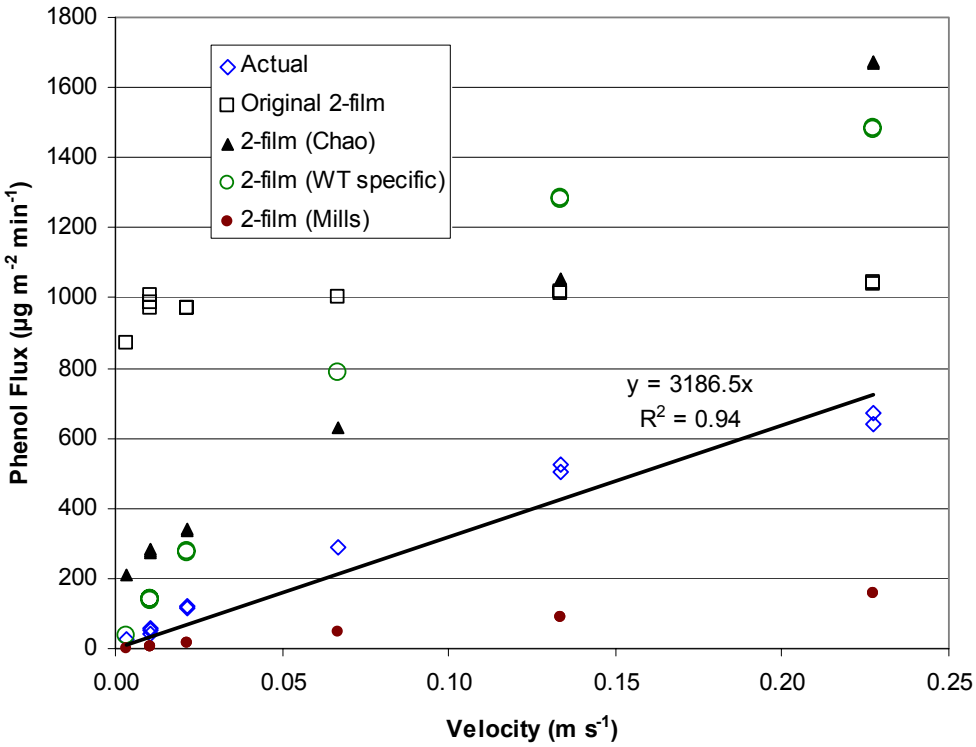

Figure 10. A comparison of actual phenol flux vs. various two-film model flux predictions for a 200 mg/L phenol in water solution. All two-film predictions on this graph were calculated using a Henry's law constant of 2.6E-05.

The actual phenol flux was bound on the lower end by the Mills velocity prediction, and on the upper end by the Chao velocity prediction (Figure 10). However, it should be noted that all of the above two-film calculations were based on the published Henry's Law constant of 2.6E-05 for phenol (from Hudson and Ayoka, 2008a).

Given that the two-film model is highly dependent on the Henry's law constant, the Henry's law constant was adjusted to obtain as close a match as possible with the actual phenol flux. The two-film model with the wind-tunnel specific k_G^R correction was found to have the best match with the actual phenol flux with a Henry's law constant of 1.21E-05 at the laboratory temperature of 21.1°C (294.3 K) (Figure 11). This is in the range of published Henry's law constants for phenol (Sander, 1999).

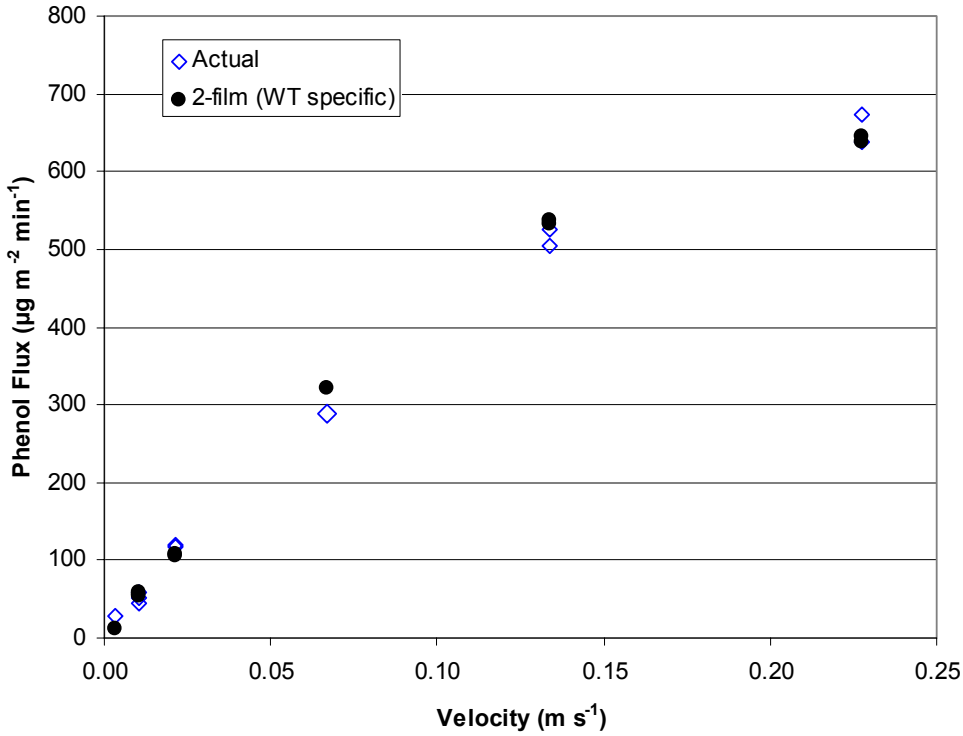

Figure 11. A comparison of actual phenol flux vs. two-film modeled flux using the wind-tunnel specific k_G^R and a dimensionless Henry's law constant of 1.21E-05 at 21.1°C.

A comparison of the models revealed several important facts. First, a velocity correction is definitely necessary to accurately represent the effects of wind speed on the flux of compounds like phenol with small Henry's law constants. Second, the accuracy of the two-film model is highly dependent on the Henry's law constant. Third, the two-film model with wind-tunnel specific k_G^R and laboratory determined Henry's law constant can accurately predict actual VOC flux.

Temperature Effects on Henry's Law Constants and Two-Film Modeled Fluxes

Henry's law constants vary with temperature, and as such the flux will vary with temperature. Sander (1999) presented the following formula for describing Henry's law as a function of temperature (T):

$$k_H = k_H^{\Theta} \exp\left(\frac{-\Delta_{sol} H}{R}\left(\frac{1}{T} - \frac{1}{T^{\Theta}}\right)\right) \qquad [14]$$

Where k_H = Henry's law constant (M/atm) at temperature *T*, k_H^{Θ} is the Henry's law constant (M/atm) at standard conditions of T^{Θ} = 298.15 K, and $\frac{\Delta_{so\ln}H}{R} = \frac{-d\ln k_H}{d(1/T)}$ is the temperature dependence factor (K).

The dimensionless Henry's law constant (i.e. Eq. 7) is then calculated from k_H using:

$$H_{cc} = \frac{12.2}{k_H\ T} \qquad [15]$$

Sander (1999) presents a range of temperature dependence factors for phenol of 3600 to 7300, with an average of 5,900. Using this average temperature dependence factor, and the laboratory-measured dimensionless Henry's law constant of 1.21E-05 as the baseline H_{cc} at standard conditions for phenol, the resulting plot of how flux varies with temperature at a constant wind tunnel velocity of 0.133 m/s is shown in Figure 12.

The curve in Figure 12 can generally be divided into three temperature zones of approximate equal slope, from -20 to 5°C, 5 to 20°C, and 20 to 40°C. The slope becomes steeper as temperature increases, indicating that at warmer temperatures, a small change in temperature has a greater effect in magnitude of overall flux.

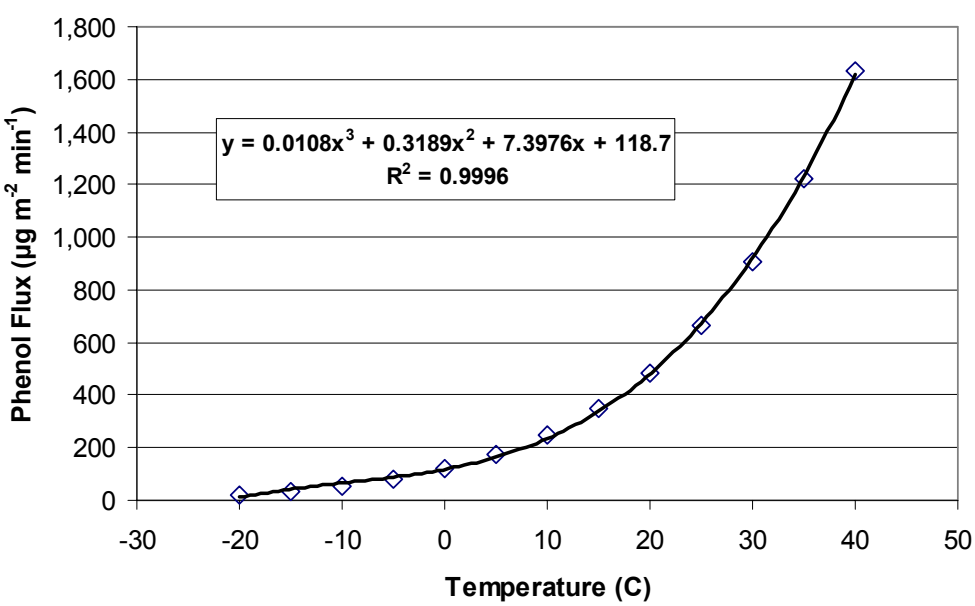

Figure 12. Plot showing the relationship between temperature and predicted phenol flux using the two film-model at a constant wind tunnel velocity of 0.133 m/s for a 200 mg/L phenol in water solution.

Conclusions

The following conclusions were drawn from this research:

1) The emission rates of eleven VOCs found at AFOs increased linearly between wind tunnel velocities of 0.003 and 0.2 m/s (corresponding to volumetric air exchange rates of 0.6 to 39 exchanges per minute) as measured at 2 cm height above the measuring surface. These results show that wind velocity affects VOC emissions from AFOs. Therefore, wind velocity effects should be included in emission factor estimations for these VOCs.

2) As shown by the two-film model and Henry's Law constants, the VOCs found at AFOs behave differently than those found at most industrial and hazardous waste sites. Emissions of VOCs found at AFOs are greatly affected by wind velocity, as opposed to those at most industrial-type and hazardous waste VOCs which are not greatly affected by wind velocity.

3) The two-film model with wind-tunnel specific k_G^R (measured from laboratory evaporation studies) and laboratory determined Henry's law constant was shown to accurately predict actual VOC flux over a range of wind velocities.

Acknowledgements

This was a collaborative project supported by the USDA-CSREES Project No. TS-2006-06009 entitled "Air Quality: Odor, Dust, and Gaseous Emissions from Concentrated Animal Feeding Operations in the Southern Great Plains."

Disclaimer

Mention of trade names or commercial products in this article is solely for the purpose of providing specific information and does not imply recommendation or endorsement by the U.S. Department of Agriculture or the Texas A&M University System.

References

Aquino, F.L., S.C. Capareda, C.B. Parnell, S. Mukhtar, R. Lacey, and B. Shaw. 2007. Comparison of partial reactive organic gases (ROG) emission factors from a dairy and beef feedlot. ASABE Paper 074006. St. Joseph, Mich.: ASABE.

Bianchi, A.P. and M.S. Varney. 1997. Volatilisation processes in wastewater treatment plants as a source of potential exposure to VOCs. *Ann. Occup. Hyg.* 41(4):437-454.

Bidleman, T.F. and L.L. McConnell. 1995. A review of field experiments to determine air-water gas exchange of persistent organic pollutants. *The Science of the Total Environment* 159:101-117.

Buonicore, A.J. and W. Davis, 1992. Air pollution engineering manual. Air and Waste Management Association, New York, NY.

Carter, W.P.L. 1994. Development of ozone reactivity scales for volatile organic compounds. *J. Air Waste Mgt. Assoc.* 44:881-899.

Chao, H.-P., J.-F. Lee, C.-K.Lee, and H.-C. Huang. 2005. An alternative method for predicting organic solute volatilization rates under gas and liquid turbulence. *Chemosphere* 59:711-720.

Cole, N.A., R.W. Todd, D.B. Parker and M.B. Rhoades. 2007. Challenges in using flux chambers to measure ammonia emissions from simulated feedlot pen surfaces and retention ponds. International Symposium on Air Quality and Waste Management for Agriculture. September 16-19, 2007. 6 pp.

Delos, C.G., W.L. Richardson, J.V. DePinto, R. Ambrose, P. Rodgers, K. Rygwelski, J. St. John, W. Shaughnessy, T. Fana, and W. Christie. 1984. Technical guidance manual for performing waste load allocations, Book II Streams and rivers, Chapter 3 Toxic substances. EPA-440/4-84-022. United States Environmental Protection Agency, Washington, DC.

Eklund, B. 1992. Practical guidance for flux chamber measurements of fugitive volatile organic emission rates. *J. Air Waste Mgt. Assoc.* 42:1583-1591.

Fowler, D., M. Coyle, C. Flechard, K. Hargreaves, E. Nemitz, R. Storeton-West, M. Sutton, and J-W, Erisman. 2001. Advances in micrometeorological methods for the measurement and interpretation of gas and particle nitrogen fluxes. *Plant and Soil* 228:117-129.

Gholson, A., J. Albritton and R. Jayanty. 1989. Evaluation of the flux chamber method for measuring volatile organic emissions from surface impoundments. EPA/600/3-89/008, U.S. Environmental Protection Agency: Research Triangle Park, North Carolina.

Gholson, A.R., J.R. Albritton and R.K.M. Jayanty. 1991. Evaluation of an enclosure method for measuring emissions of volatile organic compounds from quiescent liquid surfaces. *Environ. Sci. Technol.* 25:519-524.

Ham, J.M. 2005. Useful equations and tables in micrometeorology. In Hatfield, J.L., and Baker, J.M. (eds.). Micrometeorology in Agricultural Systems. Agronomy Monograph No. 17. American Society of Agronomy, Madison, WI.

Hudson, N. and G. A. Ayoko. 2008a. Odour sampling 1: Physical chemistry considerations. *Bioresource Technology* 99(10):3988-3992.

Hudson, N. and G. A. Ayoko. 2008b. Odour sampling 2: Comparison of physical and aerodynamic characteristics of sampling devices: A review. *Bioresource Technology* 99(10):3993-4007.

Kissel, D.E., H.L. Brewer, G. F. Arkin. 1977. Design and test of a field sampler for ammonia volatilization. *Soil Sci Soc Amer. J.* 41:1133-1138.

Lee, J-F, H-P Chao, C.T. Chiou, and M. Manes. Turbulence effects on volatilization rates of liquids and solutes. *Environ. Sci. Technol.* 38:4327-4333.

Leyris, C., J-M Guillot, J-L Fanlo and L. Pourtier. 2005. Comparison and development of dynamic flux chambers to determine odorous compound emission rates from area sources. *Chemosphere* 59:415-421.

Lindberg, S.E., H. Zhang, A. F. Vette, M.S. Gustin., M. O. Barnett and T. Kuiken. 2002. Dynamic flux chamber measurement of gaseous mercury emission fluxes over soils. Part 2: effect of flushing flow rate and verification of a two-resistance exchange interface simulation model. *Atmospheric Environment* 36:847-859.

Liss, P.S. and P.G. Slater. 1974. Flux of gases across the air-sea interface. *Nature* 247:181-184.

Meisinger, J.J., A.M. Lefcourt, and R.B. Thompson. 2001. Construction and validation of small mobile wind tunnels for studying ammonia volatilization. *Applied Eng. Agric.* 17(3): 375-381

Mills, W.B., D.B. Porcella, M.J. Ungs, S.A. Gherini, K.V. Summers, L. Mok, G.L. Rupp, G.L. Bowie, D. A. Haith. 1985. Water quality assessment : A screening procedure for toxic and conventional pollutants in surface and ground water (revised 1985) Part 1. EPA-600/6-85-002a. U.S. EPA Environmental Research Laboratory, Athens, GA.

NAS. 2003. Air emissions from animal feeding operations: Current knowledge, future needs. National Research Council of the National Academies. National Academies Press, Washington, DC.

Parker, D.B., Z. Buser, E. Caraway, Marty Rhoades, M. Olsen, K. Casey, J. Spears, G. Green. 2007. VOC concentrations downwind of beef feedlots during intense odour events. In: Proc. of the 14th IUAPPA World Congress, Brisbane, Australia. September 9-13, 2007.

Rabaud, N.E., S.E. Ebeler, L.L. Ashbaugh, and R.G. Flocchini. 2002. The application of thermal desorption GC/MS with simultaneous olfactory evaluation for the characterization and quantification of odor compounds from a dairy. *J. Agric. Food Chem.* 50:5139-5145).

Rabaud, N.E., S.E. Ebeler, L.L. Ashbaugh, and R.G. Flocchini. 2003. Characterization and quantification of odorous and non-odorous volatile organic compounds near a commercial dairy in California. *Atmos. Env.* 37:933-940.

Rhoades, M. B., D. B. Parker, N. A. Cole, R. DeOtte, B. W. Auvermann and Z. L. Perschbacher-Buser. 2005. Factors affecting ammonia emission measurements with surface isolation flux chambers. ASAE Meeting Paper No. 05-4026. St. Joseph, Mich. ASAE.

Ryden, J.C. and D. Lockyer. 1985. Evaluation of a System of Wind Tunnels for Field Studies of Ammonia Loss from Grassland through Volatilisation. *J. Sci. Food Agric.* 36: 781-788.

Sadek, S.E., J.D. Smith, A.T. Watkin and R. Gebel. Mass transfer of volatile organics from large open basins. *Environmental Progress* 15(2):82-92.

Sander, R. 1999. Compilation of Henry's Law constants for inorganic and organic species of potential importance in environmental chemistry. Version 3. Available at: http://www.mpch-mainz.mpg.de/~sander/res/henry.html

Sawyer, C.N. and P. L. McCarty. 1978. *Chemistry for environmental engineering*. 3rd ed., , New York, NY: McGraw-Hill, Inc.

Staudinger, J. and P. V. Roberts. 2001. A critical compilation of Henry's law constant temperature dependence relations for organic compounds in dilute aqueous solutions. *Chemosphere* 44:561-576.

U.S. EPA. 1995a. Air Quality: Revision to Definition of Volatile Organic Compounds--Exclusion of Acetone. 40CFR51.100(s). United States Environmental Protection Agency, Wash. DC. (http://www.epa.gov/EPA-AIR/1995/June/Day-16/pr-752.html).

U.S. EPA. 1995b. Definition and procedure for the determination of the method detection limit – Revision 1.11. 40CFR Part 136, Appendix B. United States Environmental Protection Agency, Washington, D.C.

U.S. EPA. 1999. Determination of volatile organic compounds in ambient air using active sampling onto sorbent tubes. Compendium Method TO-17. United States Environmental Protection Agency, Cincinatti, OH.

Wanninkhof, R. 1992. Relationship between wind speed and gas exchange over the ocean. *J. Geophysical Research* 97(C5):7373-7382.

Watkins, S.H., R.F. Strand, D.S. Debell, and J. Esch, Jr. 1972. Factors Influencing Ammonia Losses from Urea Applied to Northwestern Forest Soils. *Soil Sc. Soc. Am. Proc.* 36:354-357.

Whitehead, D.C. and N. Raistrick. 1991. Effects of some environmental factors on ammonia volatilization from simulated livestock urine applied to soil. *Biol-Fertil-Soils* 11(4): 279-284.

Wright, D.W., D.K. Eaton, L.T. Nielsen, F.W. Kuhrt, J.A. Koziel, J.P. Spinhirne and D.B. Parker. 2005. Multidimensional gas chromatography-olfactometry for identification and prioritization of malodors from confined animal feeding operations. *J. Agric. Food Chem.* 53:8663-8672.

Zahn, J.A., J. L. Hatfield, Y.S. Do, A.A. DiSpirito, D.A. Laird and R.L. Pfeiffer. 1997. Characterization of volatile organic emissions and wastes from a swine production facility. *J. Environ. Qual.* 26:1687-1696.

Zhang, H., S.E. Lindberg, M.O. Barnett, A.F. Vette, and M.S. Gustin. 2002. Dynamic flux chamber measurement of gaseous mercury emission fluxes over soils. Part 1: simulation of gaseous mercury emissions from soils using a two-resistance exchange interface model. *Atmospheric Environment* 36:835-846.